JBC ARTICLE

A repressive role of enhancer of zeste homolog 2 in 11β-hydroxysteroid dehydrogenase type 2 expression in the human placenta

Received for publication, November 1, 2016, and in revised form, March 2, 2017 Published, Papers in Press, March 16, 2017, DOI 10.1074/jbc.M116.765800

Rujuan Zuo[‡§], **Xiaohui Liu**[¶], **Wangsheng Wang**[‡§], **Wenjiao Li**[‡§], **Hao Ying**[¶], **and Kang Sun**[‡§1]

From the [‡]*Center for Reproductive Medicine, Ren Ji Hospital, School of Medicine, Shanghai Jiao Tong University, Shanghai 200135, China, the* [§]*Shanghai Key Laboratory for Assisted Reproduction and Reproductive Genetics, Shanghai 200135, China, and the* [¶]*Shanghai First Maternity and Infant Hospital, School of Medicine, Tongji University, Shanghai 200135, China*

Edited by John M. Denu

The expression of 11β-hydroxysteroid dehydrogenase type 2 (11β-HSD2), which acts as a placental glucocorticoid barrier, is silenced in cytotrophoblasts but substantially up-regulated during syncytialization. However, the repressive mechanism of 11β-HSD2 expression before syncytialization and how this repression is lifted during syncytialization remain mostly unresolved. Here we found that enhancer of zeste homolog 2 (EZH2) accounts for the silence of 11β-HSD2 expression via trimethylation of histone H3 lysine 27 at the promoter of the 11β-HSD2 gene. Further studies revealed that, upon syncytialization, human chorionic gonadotropin reduced the phosphorylation of retinoblastoma protein (pRB) via activation of the cAMP/PKA pathway, which sequesters E2F transcription factor 1 (E2F1), the transcription factor for EZH2 expression. As a result of inactivation of the pRB-E2F1-EZH2 pathway, the repressive marker trimethylation of histone H3 lysine 27 at the 11β-HSD2 promoter is removed, which leads to the robust expression of 11β-HSD2 during syncytialization.

In the human placenta, syncytialization is a differentiating process whereby mononuclear cytotrophoblasts fuse into multinuclear syncytiotrophoblasts (1, 2). The syncytialized trophoblasts, by covering the placental villi that immerse in the maternal blood, form a nutrient exchange interface between mother and fetus as well as a frontline defense for the fetus against harmful substances from the maternal side (1). One such defensive role of syncytiotrophoblasts is to provide a barrier against maternal glucocorticoids that is about 10-fold higher than that on the fetal side (3). Although appropriate amounts of glucocorticoids facilitate the maturation of fetal organs, accumulating evidence has indicated that excessive glucocorticoids not only compromise fetal growth but also program the development of chronic diseases during the postnatal period (3, 4). Therefore, this placental glucocorticoid barrier is critical for the normal development of the fetus. The establishment of the placental glucocorticoid barrier depends on the robust induction of 11β-hydroxysteroid dehydrogenase type 2 (11β-HSD2),[2] an exclusive oxidase catalyzing the conversion of biologically active cortisol into inactive cortisone, during syncytialization (4–6). Intriguingly, as the precursors for syncytiotrophoblasts, cytotrophoblasts express very little 11β-HSD2 (6, 7). It remains obscure which strategy is adopted by cytotrophoblasts to suppress 11β-HSD2 expression and how this suppression is lifted during syncytialization. Elucidating these issues will provide fundamental insights into the molecular mechanism underlying the establishment of the placental glucocorticoid barrier.

11β-HSD2 is encoded by the *HSD11B2* gene, which is rich in CpG islands (8). The tissue-specific expression of 11β-HSD2 is associated with the methylation state of these CpG islands, particularly in the promoter region (8). In tissues that scarcely express 11β-HSD2, *HSD11B2* promoter is highly methylated, whereas in tissues that express 11β-HSD2 abundantly such as the mineralocorticoid target organs, a low methylation rate has been revealed in the *HSD11B2* promote (8). Likewise, the CpG islands in the *HSD11B2* promoter in human placental tissue have also been found to have a low methylation frequency (8), which is supported by our findings that a low methylation rate of the *HSD11B2* promoter is maintained throughout syncytialization (6), suggesting that cytotrophoblasts may employ an alternative mechanism rather than DNA methylation in the suppression of 11β-HSD2 expression prior to syncytialization.

In addition to DNA methylation, epigenetic modifications of histones are also crucial in the regulation of gene expression by affecting chromosome functions. Among histone marks that repress gene transcription, trimethylation of histone H3 lysine 27 (H3K27me3) is a well recognized gene silencing mark (9). In addition, trimethylation of H3K27 is conducted by the enhancer of zeste homolog 2 (EZH2) and its cofactors suppressor of zeste 12 homolog (SUZ12) and embryonic ectoderm development (EED) (9). Of interest, ChIP sequencing revealed

This work was supported by National Natural Science Foundation of China Grants 31671566, 81330018, and 81601286 and National Key Basic Research Program of China Grant 2014CB943302. The authors declare that they have no conflicts of interest with the contents of this article.
This article contains supplemental Fig. S1 and Tables S1 and S2.

[1] To whom correspondence should be addressed. E-mail: sungangrenji@hotmail.com.

[2] The abbreviations used are: 11β-HSD2, 11β-hydroxysteroid dehydrogenase type 2; H3K27me3, trimethylation of histone H3 lysine 27; H3K27me2, dimethylation of histone H3 lysine 27; SUZ12, suppressor of zeste 12 homolog; EED, embryonic ectoderm development; hCG, human chorionic gonadotropin; EPZ, EPZ005687; GSK, GSK343; H3K27ac, acetylation of histone H2 lysine 27; pRB, retinoblastoma protein; Bt_2cAMP, dibutyryl cyclic AMP; Nc, negative control.

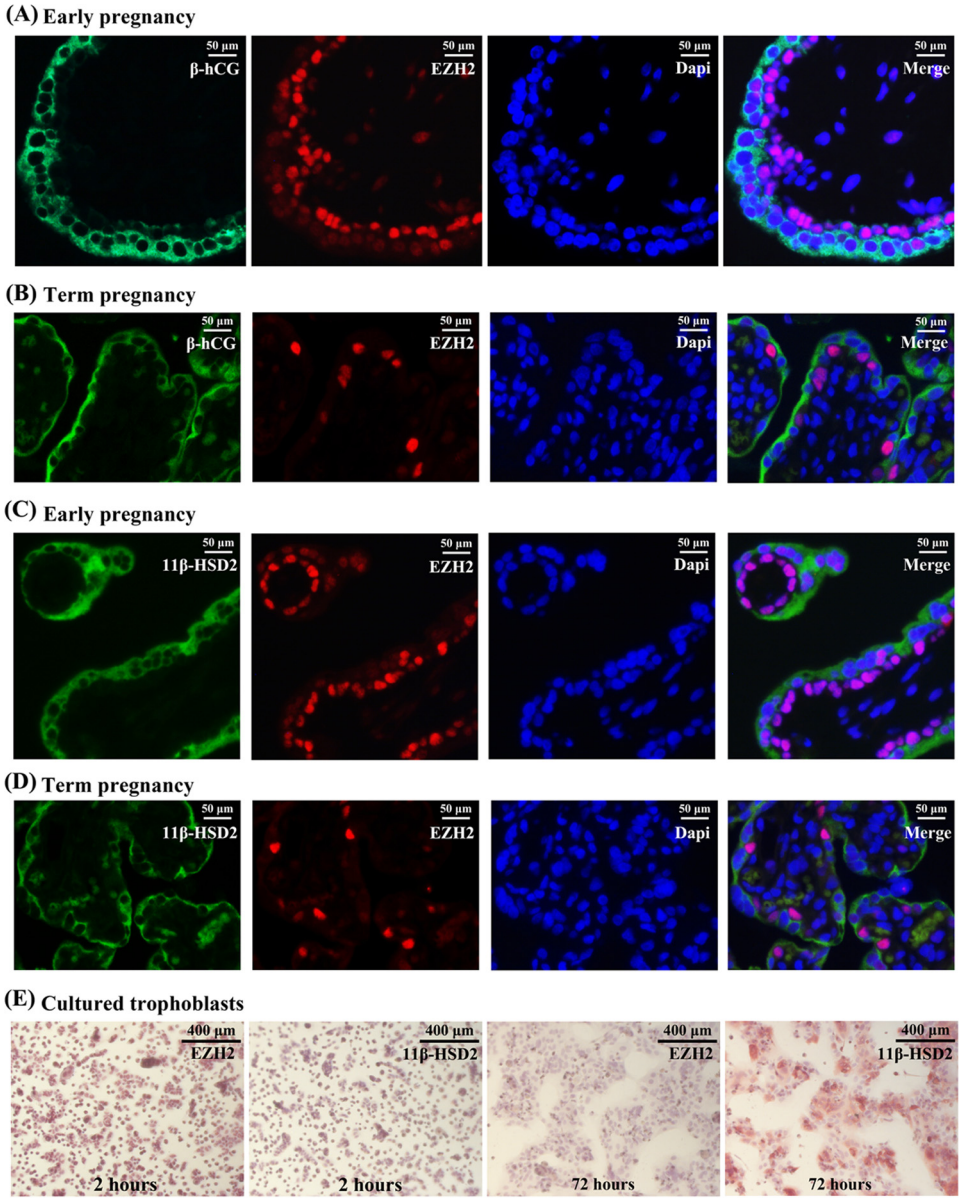

Figure 1. Distribution patterns of EZH2 in relation to 11β-HSD2 in human placental villous tissue and in trophoblasts before and after syncytialization. *A* and *B*, representative images showing intense staining of EZH2 (*red*) in the nuclei of the cytotrophoblast layer and weak staining of EZH2 in the nuclei of the syncytial layer of human chorionic villi in both early (*A*) and term (*B*) pregnancies. The syncytial layer was stained for β-hCG (*green*). Nuclei were counterstained *blue* with DAPI. $n = 5$. *C* and *D*, representative images showing a reciprocal distribution pattern of EZH2 and 11β-HSD2 in human chorionic villi in both early (*C*) and term (*D*) pregnancies. EZH2 staining (*red*) is detected mainly in cytotrophoblasts, whereas 11β-HSD2 (*green*) is found in the syncytial layer. Nuclei were counterstained *blue* with DAPI. $n = 5$. *E*, representative images showing strong EZH2 staining and weak 11β-HSD2 staining in trophoblasts before syncytialization (2 h) and weak EZH2 staining and strong 11β-HSD2 staining in trophoblasts after syncytialization (72 h). The cells were counterstained with hematoxylin. $n = 5$.

that *HSD11B2* is among the genes that are immunoprecipitated by an antibody against EZH2 in several cell lines (10–12). Our preliminary data revealed that syncytialization caused a dramatic decrease in EZH2 expression and a robust increase in 11β-HSD2 expression reciprocally in human trophoblasts. In light of the prominent role of EZH2-mediated methylation of H3K27 in gene silencing and the fact that CpG domains commonly recruit EZH2 (13, 14), it is feasible to propose that 11β-HSD2 expression might be repressed via EZH2-mediated trimethylation of H3K27 in the cytotrophoblasts and that this repressive mark might be removed as a consequence of down-regulation of EZH2 expression by the factors produced during syncytialization. Here we tested this hypothesis by using human villous tissues obtained from both early and term pregnancies.

Results

Changes in EZH2 and 11β-HSD2 abundance during syncytialization

Initially, immunofluorescent staining was conducted to examine whether EZH2 in the villous tissue manifested a unique distribution pattern. The identity of syncytiotrophoblasts was illustrated with staining for the β subunit of hCG (β-hCG), a well recognized marker for syncytiotrophoblasts

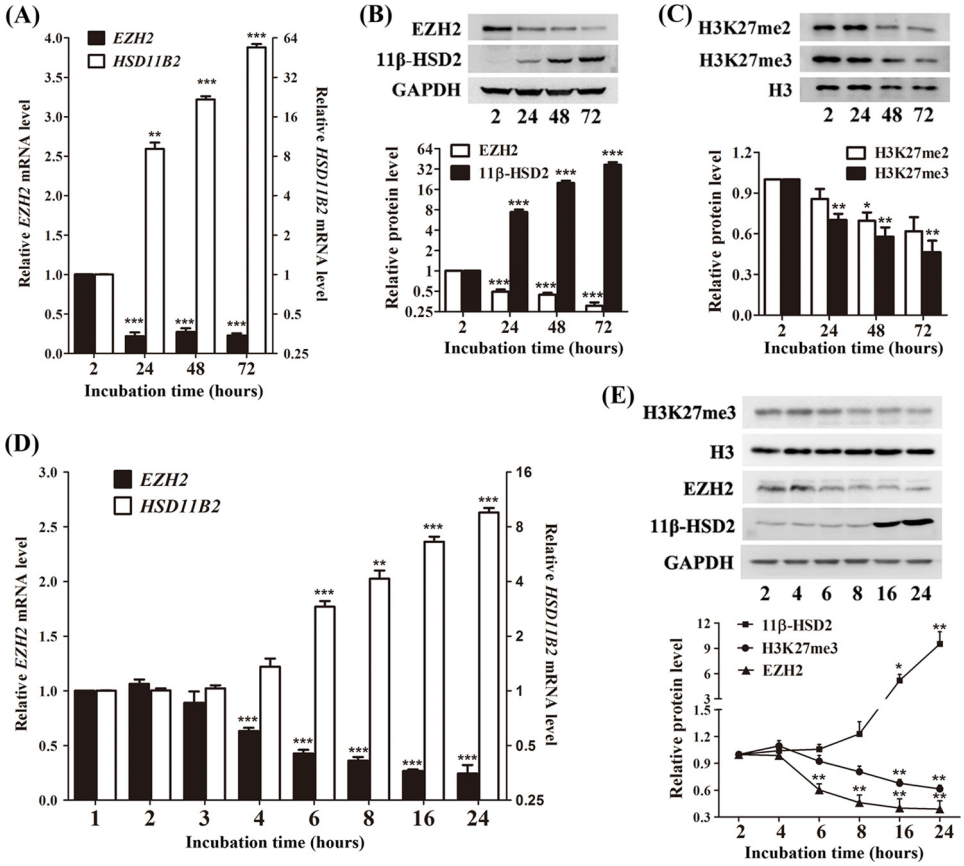

Figure 2. Time course changes in EZH2 in relation to 11β-HSD2 and H3K27me3 during syncytialization. *A*, changes in the mRNA abundance of *EZH2* (*black columns*, $n = 5$) and *HSD11B2* (*white columns*, $n = 3$) during 72 h of syncytialization process of trophoblasts. *B*, changes in the protein abundance of EZH2 ($n = 7$) and 11β-HSD2 ($n = 5$) during 72 h of the syncytialization process. *C*, decreases in the abundance of H3K27me2 ($n = 3$) and H3K27me3 ($n = 4$) during 72 h of the syncytialization process. *D*, reciprocal changes in the mRNA abundance of *EZH2* (*black columns*) and *HSD11B2* (*white columns*) during the first 24 h of culture. Significant down-regulation of *EZH2* appeared ahead of the up-regulation of *HSD11B2*. $n = 3$. *E*, time course changes in the protein abundance of EZH2, H3K27me3, and 11β-HSD2 during the first 24 h of culture. The reduction in EZH2 appeared ahead of the changes in H3K27me3 and 11β-HSD2. $n = 4$. *, $p < 0.05$; **, $p < 0.01$; ***, $p < 0.001$ against 1 h or 2 h.

(2). In the villous tissue obtained from both early (Fig. 1*A*) and term (Fig. 1*B*) pregnancies, EZH2 was localized dominantly in the nuclei of cytotrophoblasts, and weak staining for EZH2 was observed in the nuclei of syncytiotrophoblasts and interstitial cells, suggesting that EZH2 functions mainly in the nuclei of cytotrophoblasts. Further examination of the distribution of EZH2 in relation to 11β-HSD2 in villous tissue collected from both early (Fig. 1*C*) and term (Fig. 1*D*) pregnancies revealed that the cytotrophoblast layer with little staining for 11β-HSD2 was intensely stained for EZH2, whereas the syncytial layer carrying intense staining for 11β-HSD2 was faintly stained for EZH2.

To observe the dynamic change of EZH2 expression in relation to 11β-HSD2 expression during syncytialization, we employed primary human cytotrophoblasts, which are capable of fusing spontaneously into large syncytial clumps *in vitro* (15). Immunocytochemical staining revealed that strong EZH2 staining was detected in the nuclei of trophoblasts before syncytialization (2 h) and became rather weak after syncytialization (72 h). On the contrary, the 11β-HSD2 staining signal, which was observed sparsely in cytotrophoblasts, became rather intense in syncytiotrophoblasts (Fig. 1*E*). Further studies demonstrated that the abundance of EZH2 mRNA and protein was dramatically decreased in trophoblasts after 24-h incubation, which was accompanied by a concurrent increase in 11β-HSD2 mRNA and protein abundance as well as a simultaneous reduction in H3K27me3 and H3K27me2 (Fig. 2, *A*–*C*). A time course study within the first 24 h of cell culture revealed that the change in EZH2 abundance occurred ahead of the changes in H3K27me3 and 11β-HSD2 abundance (Fig. 2, *D* and *E*). These data suggest that a negative correlation between EZH2 and 11β-HSD2 expression exists in trophoblasts and that the down-regulation of EZH2 expression is very likely the causative factor for the up-regulation of 11β-HSD2 expression by removing H3K27me3 from the *HSD11B2* promoter during syncytialization.

The role of EZH2 in the regulation of 11β-HSD2 expression in human placental trophoblasts

To examine the role of EZH2 in the regulation of 11β-HSD2 expression in trophoblasts, we first determined by ChIP assays whether EZH2 is enriched at the *HSD11B2* promoter in human cytotrophoblasts. We found that the enrichment of EZH2 as well as SUZ12 and EED, the cofactors for EZH2, was significantly more abundant at the *HSD11B2* promoter in trophoblasts before syncytialization compared with that in syncytiotrophoblasts. The changes in H3K27me3 enrichment at the *HSD11B2* promoter manifested a pattern similar to that of

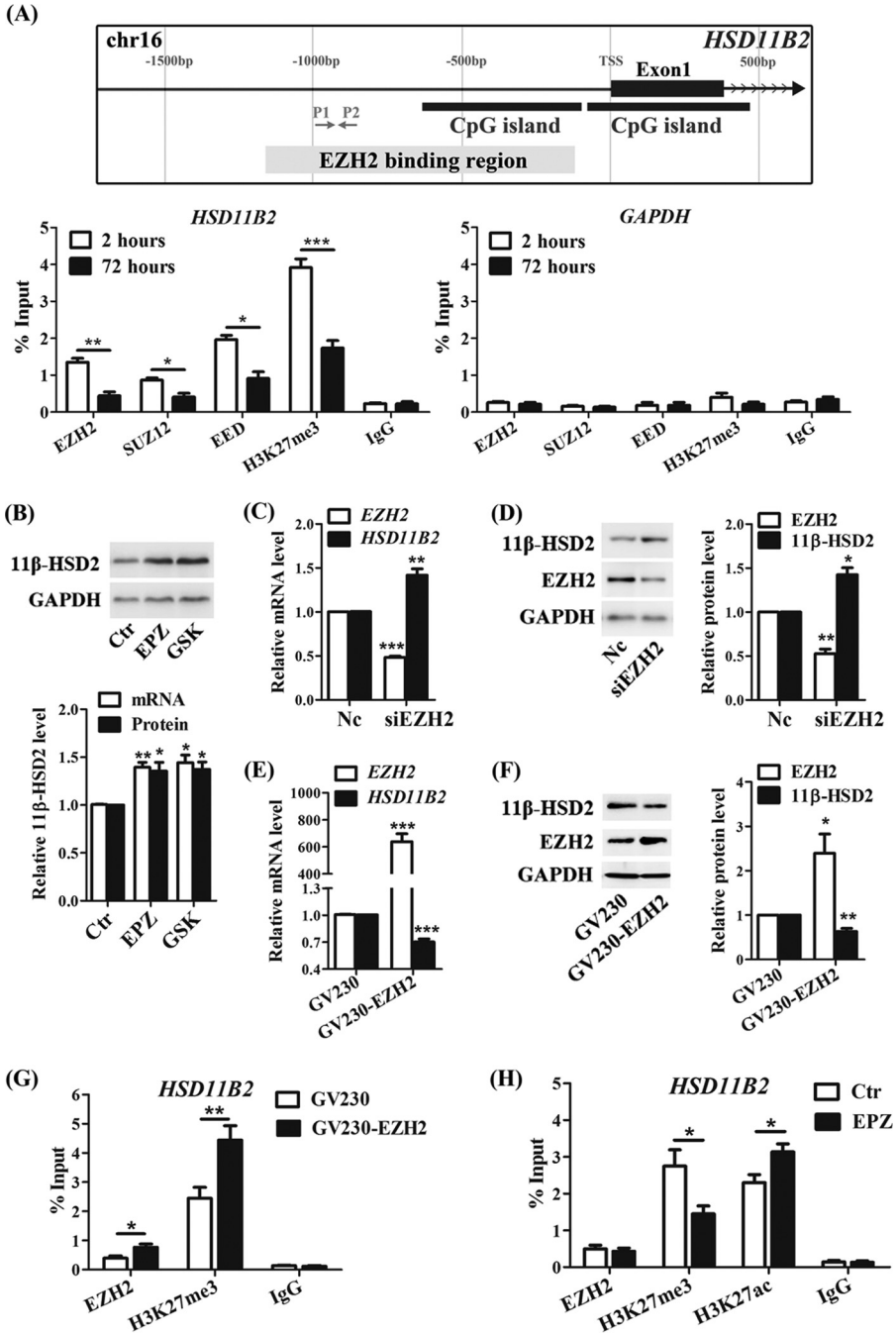

Figure 3. The effect of EZH2 on the expression of 11β-HSD2 in human placental trophoblasts. *A*, *bottom panel*, ChIP assay demonstrating the abundant enrichment of EZH2 ($n = 5$), EED ($n = 3$), SUZ12 ($n = 3$), and H3K27me3 ($n = 5$) at the promoter of *HSD11B2* (*left*) and low enrichment of these proteins at the promoter of the housekeeping gene *GAPDH* (*right*). This enrichment at the promoter of *HSD11B2* but not at the promoter of *GAPDH* was reduced significantly after syncytialization of trophoblasts. Preimmune IgG ($n = 5$) served as the negative control. *Top panel*, the location of CpG islands, the putative EZH2 binding region, and the spanning region of primers used for ChIP in the *HSD11B2* promoter. *TSS*, transcription start site. *B*, treatment with EPZ (20 μM) or GSK (10 μM), inhibitors for EHZ2, for 48 h significantly up-regulated the amounts of 11β-HSD2 mRNA and protein in trophoblasts. $n = 4$. *Ctr*, control. *C* and *D*, siRNA-mediated knockdown of EZH2 (*siEZH2*) significantly up-regulated the abundance of 11β-HSD2 mRNA ($n = 6$) and protein ($n = 4$). Randomly scrambled siRNA served as a negative control (Nc). *E* and *F*, overexpressing EZH2 for 48 h decreased the abundance of 11β-HSD2 mRNA ($n = 5$) and protein ($n = 6$). The empty vector GV230 served as a control. *G*, ChIP assays showed that the enrichment of both EZH2 and H3K27me3 at the *HSD11B2* promoter was increased by overexpression of EZH2 for 48 h. $n = 4$. *H*, ChIP assays showed that treatment with EPZ (20 μM, 48 h) decreased the enrichment of H3K27me3 but increased the enrichment of H3K27ac at the *HSD11B2* promoter. $n = 4$. *, $p < 0.05$; **, $p < 0.01$; ***, $p < 0.001$ against 2 h (*A*), control (*B* and *H*), Nc (*C* and *D*), or GV230 (*E*–*G*).

EZH2 during syncytialization. Studies of the enrichment of these proteins at the housekeeping gene *GAPDH* were performed in parallel as a negative control (Fig. 3*A*).

To further clarify the role of EZH2 in the regulation of 11β-HSD2 expression, 2 h after plating, cytotrophoblasts were treated with EPZ005687 (EPZ) or GSK343 (GSK), the specific antagonists for EZH2 (16, 17), for 48 h. EPZ or GSK treatment increased the abundance of both 11β-HSD2 mRNA and protein significantly (Fig. 3*B*). Consistently, siRNA-mediated knockdown of EZH2 also increased the

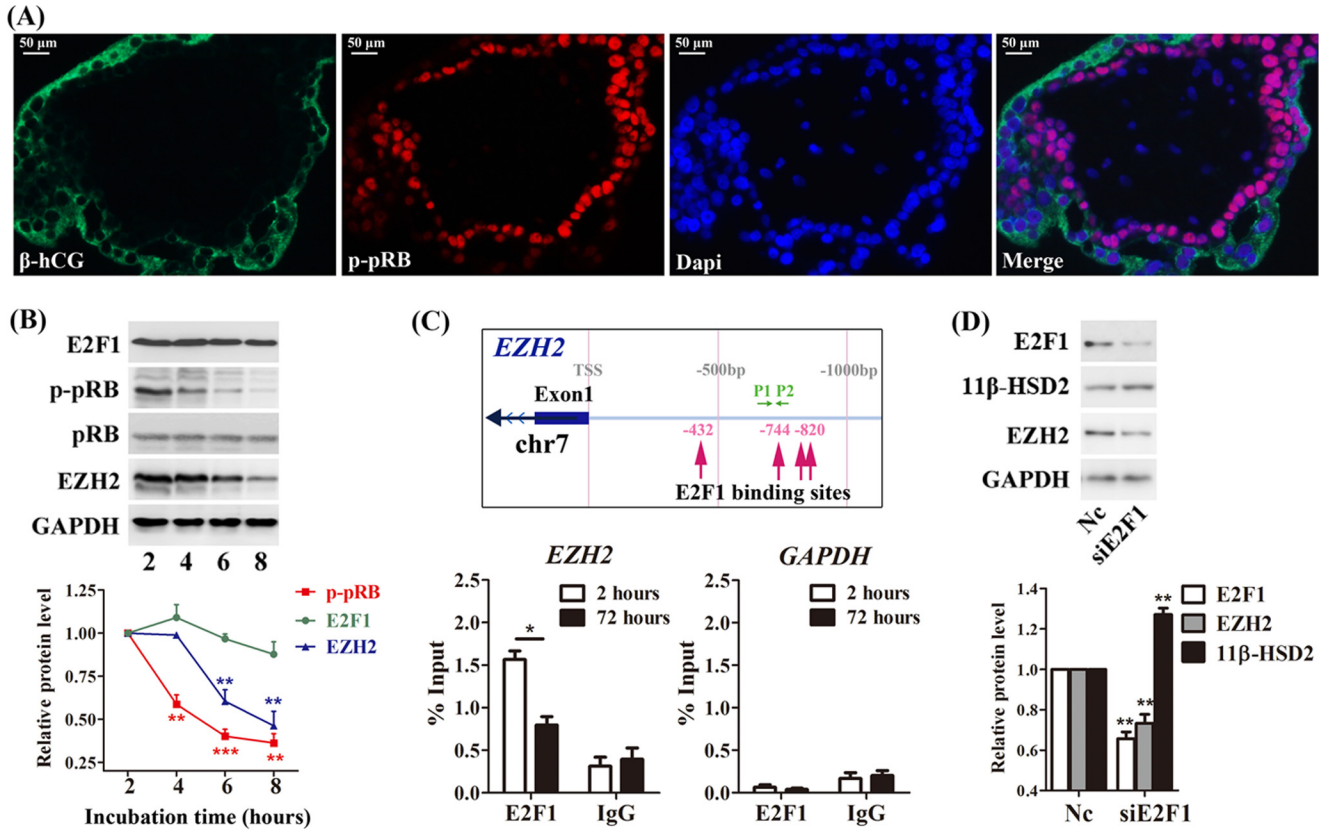

Figure 4. The role of the pRB-E2F1 pathway in EZH2-mediated repression of 11β-HSD2 expression in trophoblasts. *A*, representative immunofluorescence images showing the intense staining of p-pRB (*red*) in the nuclei of cytotrophoblasts and weak staining in the nuclei of the syncytial layer of human chorionic villi at early pregnancy. The syncytial layer was labeled with β-hCG staining (*green*). Nuclei were counterstained *blue* with DAPI. $n = 5$. *B*, time course changes of phosphorylated pRB in relation to E2F1 and EZH2 during the initial 8 h of culture. There was no significant change in E2F1 abundance, whereas p-pRB abundance was down-regulated 2 h ahead of the reduction in EZH2 abundance. $n = 4$. *C*, *bottom panel*, ChIP assays showed that the enrichment of E2F1 at the *EZH2* promoter but not at the *GAPDH* promoter was decreased significantly after syncytialization. Preimmune IgG served as a negative control. *Top panel*, the putative E2F1 binding sites in the *EZH2* promoter and the spanning region of primers used for the ChIP assay. *TSS*, transcription start site. $n = 5$. *D*, siRNA-mediated knockdown of E2F1 significantly decreased EZH2 and increased 11β-HSD2 protein abundance. Randomly scrambled siRNA served as the Nc. $n = 4$. *, $p < 0.05$; **, $p < 0.01$; ***, $p < 0.001$ against 2 h (*B* and *C*) or Nc (*D*).

amounts of 11β-HSD2 mRNA and protein in trophoblasts (Fig. 3, *C* and *D*), whereas overexpressing EZH2 for 48 h significantly decreased 11β-HSD2 mRNA and protein abundance in trophoblasts (Fig. 3, *E* and *F*). The ChIP assay showed that overexpression of EZH2 significantly enhanced the enrichment of EZH2 and H3K27me3 at the *HSD11B2* promoter in trophoblasts (Fig. 3*G*). Accordingly, EPZ005687 treatment decreased the enrichment of H3K27me3 significantly, but not EZH2 *per se*, at the *HSD11B2* promoter (Fig. 3*H*), whereas the enrichment of H3K27 acetylation (H3K27ac), a histone marker associated with the up-regulation of *HSD11B2* transcription during syncytialization (5), was increased significantly at the *HSD11B2* promoter (Fig. 3*H*). As removal of the methyl group is a prerequisite for histone acetylation (18), we assume that the reduction in H3K27me3 enrichment at the *HSD11B2* promoter may predispose H3K27 to acetylation during syncytialization. Altogether, these data indicate that EZH2-mediated H3K27 methylation is responsible for the repression of 11β-HSD2 expression before syncytialization and that this repression is lifted via down-regulation of EZH2 expression during syncytialization.

Involvement of the pRB-E2F1 pathway in the regulation of placental EZH2 expression

Previous studies in tumor cells have demonstrated that EZH2 is under the transcriptional regulation of E2F transcription factor 1 (E2F1) (19). The transcriptional activity of E2F1 is suppressed when it is bound to retinoblastoma protein (pRB). When pRB is phosphorylated, E2F1 becomes free and regains its transcriptive activity (19, 20). Consistent with the pattern of EZH2 localization in villous tissue, stronger staining for phosphorylated pRB (p-pRB) was observed in cytotrophoblasts compared with syncytiotrophoblasts in early pregnancy (Fig. 4*A*). The time course study within the first 8 h showed that the reduction in p-pRB abundance occurred before the reduction in EZH2 abundance, although the abundance of E2F1 was barely changed (Fig. 4*B*). These data suggest that the amount of E2F1 bound to pRB is increased, which may account for the reduced transcriptional activity of E2F1 and the subsequent attenuation of EZH2 expression during syncytialization.

The role of E2F1 in the regulation of EZH2 expression was further examined in trophoblasts. A ChIP assay showed that the enrichment of E2F1 at the *EZH2* promoter was more abundant before syncytialization than after syncytialization (Fig. 4*C*).

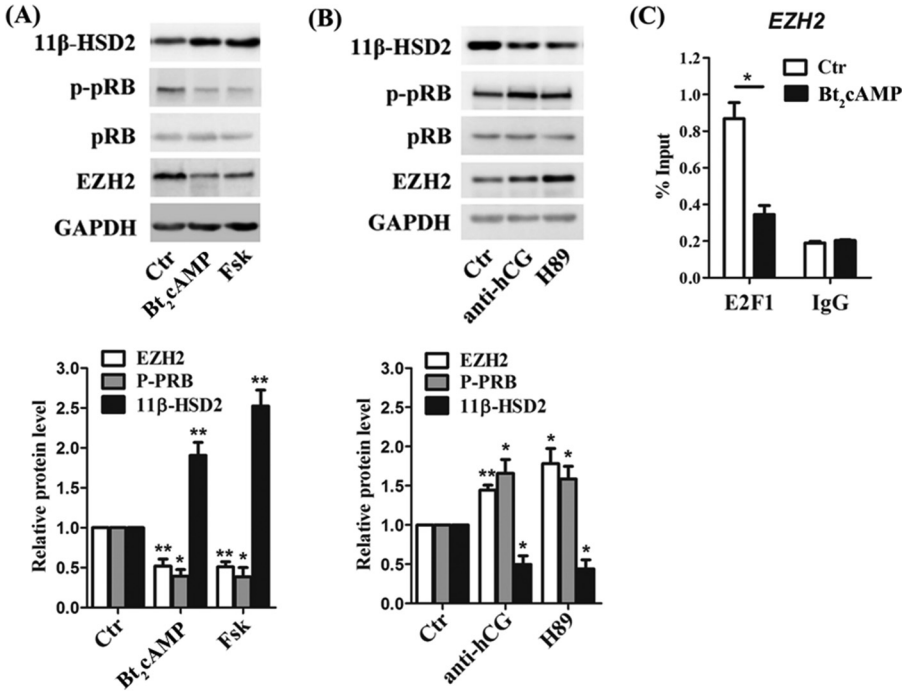

Figure 5. The human CG-activated cAMP-PKA pathway in the lift of EZH2-mediated repression on 11β-HSD2 expression during syncytialization. *A*, treatment of trophoblasts with Bt_2cAMP (200 μM) or forskolin (*Fsk*, 100 μM) for 24 h significantly decreased the amounts of p-pRB ($n = 3$) and EZH2 ($n = 5$) protein and increased 11β-HSD2 protein ($n = 5$). *Ctr*, control. *B*, treatment of trophoblasts with β-hCG antibody (*anti-hCG*, 1:100) or the PKA inhibitor H89 (20 μM) for 24 h significantly increased the abundance of p-pRB and EZH2 protein and reduced the abundance of 11β-HSD2 protein. $n = 4$. *C*, the ChIP assay demonstrated decreased enrichment of E2F1 at the *EZH2* promoter upon stimulation by Bt_2cAMP (200 μM, 24 h). Preimmune IgG served as the negative control. $n = 4$. *, $p < 0.05$; **, $p < 0.01$ against the control.

Knockdown of E2F1 expression by siRNA significantly reduced EZH2 abundance but increased 11β-HSD2 abundance in trophoblasts (Fig. 4*D*). These data indicate that E2F1 is the transcription factor that stimulates EZH2 expression in cytotrophoblasts and that, during syncytialization, E2F1 is sequestered by pRB, resulting in decreased expression of EZH2.

The human CG-activated cAMP/PKA pathway is responsible for the removal of repression on 11β-HSD2 expression during syncytialization

It is well recognized that the hCG-activated cAMP/PKA pathway is pivotal for syncytialization (2, 21). Moreover, the cAMP/PKA pathway can attenuate pRB phosphorylation in some tumor cells (22, 23). Therefore, we hypothesized that the hCG-activated cAMP/PKA pathway might be the upstream signal that directs the down-regulation of EZH2 expression during syncytialization. We found that treatment with dibutyryl cyclic AMP (Bt_2cAMP), an analogue of cAMP, or forskolin, an activator for adenylyl cyclase, decreased the amounts of phosphorylated pRB and EZH2 while increasing 11β-HSD2 abundance (Fig. 5*A*). Consistently, neutralization of hCG with β-hCG antibody or inhibition of PKA with H89 significantly increased the abundance of p-pRB and EZH2 while decreasing 11β-HSD2 abundance (Fig. 5*B*). Despite an unaltered abundance of total E2F1 by manipulation of the hCG-cAMP-PKA pathway (supplemental Fig. S1), Bt_2cAMP treatment significantly reduced the enrichment of E2F1 at the *EZH2* promoter (Fig. 5*C*), which is possibly due to the reduction in the amount of active E2F1. These data suggest that the hCG-activated cAMP-PKA pathway is the upstream signal that causes the down-regulation of EZH2 expression via inactivation of the pRB-E2F1 pathway during syncytialization.

Discussion

This study demonstrates that EZH2 plays a repressive role in the regulation of 11β-HSD2 expression before syncytialization by way of trimethylating H3K27. We believe that the transcription factor E2F1 drives the abundant expression of EZH2 in cytotrophoblasts before syncytialization. Upon syncytialization, the marked production of hCG leads to a reduction in the phosphorylation of pRB via activation of the cAMP-PKA pathway, which decreases the level of free E2F1 and diminishes E2F1 transcriptional activity. As a result, EZH2 and H3K27me3 abundance are reduced, rendering H3K27 available for acetylation, which transforms the chromatin from a compact structure into a loose form, allowing access of the *HSD11B2* promoter to the transcription factors, thus driving the expression of 11β-HSD2 (Fig. 6). We have demonstrated previously that P300 acetylates H3K27 and that Sp1 is a transcription factor that regulates 11β-HSD2 expression in syncytiotrophoblasts (5, 6).

Our finding that the pRB-E2F1 pathway maintains EZH2 expression in cytotrophoblasts is similar to what is found in tumor cells, which adopt this signaling pathway to maintain proliferation (19, 20). Indeed, cytotrophoblasts resemble tumor cells in many aspects, and they employ similar molecular pathways in the regulation of proliferation, migration, and invasion (24). In tumor cells, exaggerated EZH2 expression is under the tight regulation of pRB-E2F1 to promote proliferation (16, 19). In human trophoblasts, when cytotrophoblasts undergo syncytialization, the cell cycle is arrested, resulting in the loss of such

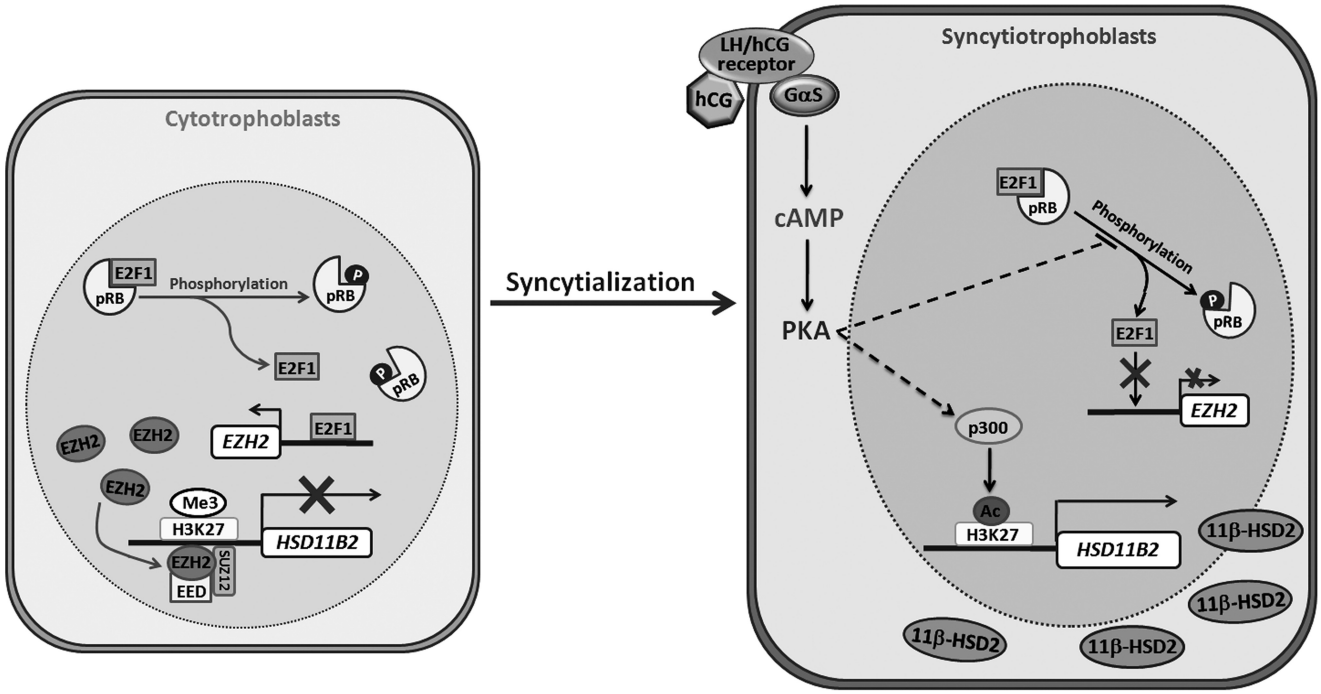

Figure 6. A schematic illustrating the mechanism that underpins the lifting of EZH2-mediated repression on 11β-HSD2 expression during syncytialization. Before syncytialization, the abundant free E2F1 as a result of pRB phosphorylation leads to the abundant expression of EZH2. By interacting with EED and SUZ12, EZH2 trimethylates H3K27 at the *HSD11B2* promoter, resulting in the repression of 11β-HSD2 expression. Upon syncytialization, the dramatic production of hCG activates the cAMP-PKA pathway, which leads to inactivation of the pRB-E2F1 pathway by decreasing the phosphorylation of pRB. A subsequent reduction in EZH2 expression results in decreased H3K27 methylation, rendering its acetylation at the *HSD11B2* promoter, which transforms the chromatin from a compact structure into a loose form, allowing access of the *HSD11B2* promoter to the transcription factors, thus driving the expression of 11β-HSD2.

tumor-like properties (24, 25), which may explain the compromised pRB-E2F1 signaling pathway and the consequent down-regulation of EZH2 expression during syncytialization. Although we are unclear about the exact genes pertinent to trophoblast proliferation that are regulated by EZH2, this study does suggest that *HSD11B2* is one of the genes that is repressed by EZH2 before syncytialization. Glucocorticoids have been reported to regulate cell proliferation in a cell context-dependent manner with anti- or pro-proliferative actions (26, 27). Whether lifting EZH2-mediated repression of 11β-HSD2 expression is related to the loss of trophoblast proliferative after syncytialization remains unclear, but one role is certainly related to the establishment of a placental glucocorticoid barrier.

In this study, we demonstrate that the cAMP-PKA pathway activated by hCG is responsible for lifting the pRB-E2F1-EZH2 pathway-mediated repression of 11β-HSD2 expression upon syncytialization. Of interest, in tumor cells, a cascade of reactions caused by cAMP signals has also been shown to be engaged in the inhibition of the expression of cyclin-dependent kinases that directly phosphorylate pRB (22, 23, 28, 29). A reduction in cyclin-dependent kinase expression decreases pRB phosphorylation, thereby restraining E2F1 from its transcriptional activity, resulting in the down-regulation of EZH2. It appears that cAMP-PKA pathway-mediated EZH2 repression may be common in both tumor and trophoblast cells, although the upstream signal to the cAMP-PKA pathway may vary. Here we found that hCG is the upstream signal to this pathway in placental trophoblasts.

Among the placental hormones that utilize the cAMP-PKA pathway in their signaling transduction, hCG is not only the first hormone secreted by trophoblasts during pregnancy but also the most abundant hormone secreted by trophoblasts upon syncytialization (1, 21). Here we found that neutralizing endogenous hCG during syncytialization increased the abundance of phosphorylated pRB and EZH2. These effects are consistent with our previous findings that hCG neutralization reduces 11β-HSD2 abundance during syncytialization (30). All of these properties and effects of hCG can well explain the reciprocal dramatic down-regulation of EZH2 and up-regulation of 11β-HSD2 upon syncytialization.

Despite the fact that the CpG islands in placental *HSD11B2* are indeed subject to the methylation modifications under adverse conditions, such as prenatal maternal anxiety (31, 32) and intrauterine growth restriction (4, 33), the findings in this study as well as in previous studies (5, 6) have provided convincing evidence for the participation of histone marks in the regulation of 11β-HSD2 expression during syncytialization. In addition to the decreases in H3K27 trimethylation, these histone marks also include increases in H3K9 and H3K27 acetylation and decreases in H3K9 dimethylation (6). Our findings are consistent with a previous study that also revealed a stronger signal for H3K27me3 in human cytotrophoblasts compared with syncytiotrophoblasts (34). Nonetheless, knockout of EZH2 or its cofactors has indeed been shown to impair the development of mouse trophoblasts (35). Taking all of these findings into consideration, we believe that histone modifications rather than DNA methylation play a dominant role in the regulation of

11β-HSD2 expression during syncytialization. This notion is in line with a report that the global expression changes of genes pertinent to the differentiation of mouse trophoblast stem cells are largely attributed to histone methylation rather than DNA methylation (36).

In conclusion, this study has revealed that EZH2-mediated H3K27 methylation represses 11β-HSD2 expression before syncytialization and that activation of the hCG-cAMP-PKA pathway upon syncytialization lifts this repression through inactivation of the pRB-E2F1-EZH2 pathway.

Experimental procedures

Collection of human placental villous tissues

Human placental villous tissues were obtained from the first trimester of gestation (6–8 weeks, $n = 5$) after painless induced abortions and from term (38–40 weeks, $n = 5$) pregnancies after elective cesarean section with written informed consent under a protocol approved by the Ethics Committee of Ren Ji Hospital, School of Medicine, Shanghai Jiao Tong University. In the case of early gestation, women with histories of spontaneous abortion and those who used contraceptives were excluded from this study. In the case of term pregnancy, women with gestational complications such as preeclampsia, fetal growth restriction, and gestational diabetes were excluded from the study. The villous tissues were fixed with formalin for immunofluorescent staining or minced for cytotrophoblast isolation.

Immunochemical staining

Immunofluorescent staining was performed on paraffin-embedded sections as described previously (37). Briefly, after deparaffination and rehydration, the sections were boiled in 10 mM sodium citrate buffer for antigen retrieval and permeabilized with PBS containing 0.4% Triton X-100. After blocking and incubation with the primary antibodies (supplemental Table S1), the sections were incubated with Alexa Fluor 488- or Alexa Fluor 594-labeled secondary antibodies (Proteintech, Rosemont, IL). Nuclei were stained with DAPI (1 μg/ml). The signals were examined under a fluorescence microscope (Zeiss).

Immunocytochemical staining was conducted on cultured trophoblasts with an avidin-biotin-peroxidase method using a Vectastain® kit (Vector Laboratories, Burlingame, CA) as described previously (5). Briefly, the cells were fixed with 4% paraformaldehyde and then permeabilized. The endogenous peroxidase activity was quenched by incubation with 3% H_2O_2. After blocking and incubation with the primary antibodies (supplemental Table S1), the cells were incubated with a biotinylated secondary antibody and then with a peroxidase/streptavidin solution. The peroxidase activity was developed by incubation with 3-amino-9-ethylcarbazole (Vector Laboratories) to produce a red-colored product. Before microscopic examination, the cells were counterstained with hematoxylin and mounted.

Isolation of human placental cytotrophoblast cells

Cytotrophoblast cells were isolated from human term placenta using a modified Kliman method as reported previously (38). Briefly, the minced tissue was digested with 0.125% trypsin (Sigma) and 0.03% DNase I (Sigma) in DMEM (Gibco). After purification using a 5–65% Percoll (GE Healthcare) gradient, cytotrophoblast cells were collected and cultured in DMEM containing 10% FBS (Biological Industries) at 37 °C in 5% CO_2 and 95% air.

Treatment of cytotrophoblast cells

Two hours after plating, the following treatments were implemented in DMEM containing 10% FBS. To examine the effects of the hCG-cAMP-PKA pathway in the regulation of EZH2 and 11β-HSD2 expression, the cells were treated with β-hCG antibody (1:100, Thermo Fisher Scientific, Fremont, CA), the cAMP analog Bt_2cAMP (200 μM, Sigma), the adenylate cyclase stimulator forskolin (100 μM, Sigma), and the PKA inhibitor H89 (20 μM, Sigma) for 24 h. To study the effects of EZH2, the cells were treated with the EZH2 antagonists EPZ005687 (20 μM, Selleckchem, Houston, TX) and GSK343 (10 μM, Selleckchem) for 48 h. To further study the role of EZH2 and E2F1, the cells were transfected with siRNA against EZH2 (sense, GAGGGAAAGUGUAUGAUAATT; antisense, UUAUCAUACACUUUCCCUCTT), E2F1 (sense, CGCUAUGAGACCUCACUGATT; antisense, UCAGUGAGGUCUCAUAGCCTG) (Gene Pharma Co., Ltd., Shanghai, China) or randomly scrambled siRNA (negative control) using Lipofectamine RNAiMAX reagent (Invitrogen) for 48 h. The efficiency of EZH2 and E2F1 knockdown was about 47.4% (Fig. 3*E*) and 34.3% (Fig. 4*D*), respectively. The role of EZH2 in regulating 11β-HSD2 expression was further studied by overexpressing EZH2 in trophoblasts. The cells were transfected with a vector, GV230, expressing EZH2 (GeneChem Co., Ltd. Shanghai, China) immediately after isolation using an electroporator at 175 V for 5 ms following a protocol described previously (6).

Extraction of RNA and quantitative real-time PCR

Total RNA was extracted using an RNA extraction kit (Omega Bio-Tek, Norcross, GA) as described previously (39). After evaluating the RNA concentration, mRNA was reverse-transcribed to cDNA using the PrimeScript® RT kit (TaKaRa, Dalian, China), and cDNA was used for quantitative real-time PCR using SYBR® Premix (TaKaRa). The primer sequences are listed in supplemental Table S2. *GAPDH* was routinely used for normalization. The relative mRNA abundance was quantified using the $2^{-\Delta\Delta Ct}$ method.

Extraction of protein and analysis with Western blotting

Whole-cell lysate protein was prepared using ice-cold radioimmune precipitation assay buffer (Active Motif, Carlsbad, CA) containing a complete protease inhibitor mixture (Roche) and phosphatase inhibitor (Active Motif). Western blotting was conducted, and the data were analyzed as described previously (37, 39). Briefly, after determination of the protein concentration with a Bradford assay, about 20 μg of protein was electrophoresed in SDS-polyacrylamide gel and transferred to a nitrocellulose membrane (Merck Millipore). After blocking and incubation with primary antibodies (supplemental Table S1), the membranes were incubated with horseradish peroxidase-

conjugated secondary antibodies (Proteintech). The band with peroxidase activity was detect by a chemiluminescence detection system (Merck Millipore) and visualized using a G-Box chemiluminescence image capture system (Syngene, Cambridge, UK). Densities were analyzed using Gel-Pro Application. The abundance of methylated H3K27 and phosphorylated pRB was expressed as the ratio of their band densities over total H3 and pRB, respectively, whereas EZH2, 11β-HSD2, and E2F1 abundance was expressed as the ratio of their band densities over GAPDH.

Chromatin immunoprecipitation assay

The chromatin immunoprecipitation assay was carried out as described previously (5, 39). Briefly, after cross-linking the proteins at chromatin DNA using 1% formaldehyde, the cells were lysed with 1% sodium dodecyl sulfate lysis buffer and sonicated to shear chromatin DNA. Sheared DNA was immunoprecipitated with antibodies (supplemental Table S1) and protein A-agarose magnetic beads (Merck Millipore). After washing the beads, reverse cross-linking, and removing the contamination of RNA and protein, the immunoprecipitated DNA was extracted using a DNA purification kit (Cwbiotech, Beijing, China) for further quantitative real-time PCR analysis. Similar amounts of sheared DNA without precipitation served as inputs. The primers for quantitative real-time PCR (supplemental Table S2) were designed to amplify the region between −843 to −978 bp of the *HSD11B2* promoter, which spans the putative EZH2 binding domain (Fig. 3*A*), and the region between −648 and −754 bp of the *EZH2* promoter, which bears the putative E2F1 binding sites (Fig. 4*C*). The primers amplifying the region between −1240 to −1436 bp in the *GAPDH* promoter were used as a negative control. The data retrieved from quantitative real-time PCR were analyzed using the following equation to indicate the abundance of the proteins enriched at the respective promoters: percent input = $100\% \times 2^{(\text{C[T] input sample} - \text{C[T] IP sample})}$.

Statistical analysis

All data are expressed as mean ± S.E. The number for each experiment indicates repeated experiments using trophoblast cells from different placentas. After examination of normal distribution, paired Student's *t* test or one-way analysis of variance followed by Newman-Keuls multiple comparisons test was used where appropriate to assess the differences. Significance was set at $p < 0.05$.

Author contributions—R. Z. and K. S. designed the study and wrote the manuscript. R. Z., X. L., and W. W. performed the experiments. W. L. and H. Y. collected the clinical samples and information.

Acknowledgments—We thank Dr. Dev Sooranna (Imperial College London) for editing the manuscript.

References

1. Huppertz, B., and Borges, M. (2008) Placenta trophoblast fusion. *Methods Mol. Biol.* **475,** 135–147
2. Costa, M. A. (2016) Scrutinising the regulators of syncytialization and their expression in pregnancy-related conditions. *Mol. Cell. Endocrinol.* **420,** 180–193
3. Moisiadis, V. G., and Matthews, S. G. (2014) Glucocorticoids and fetal programming part 1: outcomes. *Nat. Rev. Endocrinol.* **10,** 391–402
4. Togher, K. L., O'Keeffe, M. M., Khashan, A. S., Gutierrez, H., Kenny, L. C., and O'Keeffe, G. W. (2014) Epigenetic regulation of the placental HSD11B2 barrier and its role as a critical regulator of fetal development. *Epigenetics* **9,** 816–822
5. Li, J., Wang, W., Liu, C., Wang, W., Li, W., Shu, Q., Chen, Z. J., and Sun, K. (2013) Critical role of histone acetylation by p300 in human placental 11β-HSD2 expression. *J. Clin. Endocrinol. Metab.* **98,** E1189–1197
6. Li, J. N., Ge, Y. C., Yang, Z., Guo, C. M., Duan, T., Myatt, L., Guan, H., Yang, K., and Sun, K. (2011) The Sp1 transcription factor is crucial for the expression of 11β-hydroxysteroid dehydrogenase type 2 in human placental trophoblasts. *J. Clin. Endocrinol. Metab.* **96,** E899–907
7. Sun, K., Yang, K., and Challis, J. R. (1997) Differential expression of 11 β-hydroxysteroid dehydrogenase types 1 and 2 in human placenta and fetal membranes. *J. Clin. Endocrinol. Metab.* **82,** 300–305
8. Alikhani-Koopaei, R., Fouladkou, F., Frey, F. J., and Frey, B. M. (2004) Epigenetic regulation of 11 β-hydroxysteroid dehydrogenase type 2 expression. *J. Clin. Invest.* **114,** 1146–1157
9. Hublitz, P., Albert, M., and Peters, A. H. (2009) Mechanisms of transcriptional repression by histone lysine methylation. *Int. J. Dev. Biol.* **53,** 335–354
10. Gerstein, M. B., Kundaje, A., Hariharan, M., Landt, S. G., Yan, K. K., Cheng, C., Mu, X. J., Khurana, E., Rozowsky, J., Alexander, R., Min, R., Alves, P., Abyzov, A., Addleman, N., Bhardwaj, N., *et al.* (2012) Architecture of the human regulatory network derived from ENCODE data. *Nature* **489,** 91–100
11. Wang, J., Zhuang, J., Iyer, S., Lin, X. Y., Greven, M. C., Kim, B. H., Moore, J., Pierce, B. G., Dong, X., Virgil, D., Birney, E., Hung, J. H., and Weng, Z. (2013) Factorbook.org: a Wiki-based database for transcription factor-binding data generated by the ENCODE consortium. *Nucleic Acids Res.* **41,** D171–176
12. Wang, J., Zhuang, J., Iyer, S., Lin, X., Whitfield, T. W., Greven, M. C., Pierce, B. G., Dong, X., Kundaje, A., Cheng, Y., Rando, O. J., Birney, E., Myers, R. M., Noble, W. S., Snyder, M., and Weng, Z. (2012) Sequence features and chromatin structure around the genomic regions bound by 119 human transcription factors. *Genome Res.* **22,** 1798–1812
13. Mendenhall, E. M., Koche, R. P., Truong, T., Zhou, V. W., Issac, B., Chi, A. S., Ku, M., and Bernstein, B. E. (2010) GC-rich sequence elements recruit PRC2 in mammalian ES cells. *PLoS Genet.* **6,** e1001244
14. Hunkapiller, J., Shen, Y., Diaz, A., Cagney, G., McCleary, D., Ramalho-Santos, M., Krogan, N., Ren, B., Song, J. S., and Reiter, J. F. (2012) Polycomb-like 3 promotes polycomb repressive complex 2 binding to CpG islands and embryonic stem cell self-renewal. *PLoS Genet.* **8,** e1002576
15. Kliman, H. J., Nestler, J. E., Sermasi, E., Sanger, J. M., and Strauss, J. F., 3rd. (1986) Purification, characterization, and *in vitro* differentiation of cytotrophoblasts from human term placentae. *Endocrinology* **118,** 1567–1582
16. Knutson, S. K., Wigle, T. J., Warholic, N. M., Sneeringer, C. J., Allain, C. J., Klaus, C. R., Sacks, J. D., Raimondi, A., Majer, C. R., Song, J., Scott, M. P., Jin, L., Smith, J. J., Olhava, E. J., Chesworth, R., *et al.* (2012) A selective inhibitor of EZH2 blocks H3K27 methylation and kills mutant lymphoma cells. *Nat. Chem. Biol.* **8,** 890–896
17. McCabe, M. T., Ott, H. M., Ganji, G., Korenchuk, S., Thompson, C., Van Aller, G. S., Liu, Y., Graves, A. P., Della Pietra, A., 3rd, Diaz, E., LaFrance, L. V., Mellinger, M., Duquenne, C., Tian, X., Kruger, R. G., *et al.* (2012) EZH2 inhibition as a therapeutic strategy for lymphoma with EZH2-activating mutations. *Nature* **492,** 108–112
18. Pasini, D., Malatesta, M., Jung, H. R., Walfridsson, J., Willer, A., Olsson, L., Skotte, J., Wutz, A., Porse, B., Jensen, O. N., and Helin, K. (2010) Characterization of an antagonistic switch between histone H3 lysine 27 methylation and acetylation in the transcriptional regulation of Polycomb group target genes. *Nucleic Acids Res.* **38,** 4958–4969
19. Bracken, A. P., Pasini, D., Capra, M., Prosperini, E., Colli, E., and Helin, K. (2003) EZH2 is downstream of the pRB-E2F pathway, essential for proliferation and amplified in cancer. *EMBO J.* **22,** 5323–5335
20. Duronio, R. J., and Xiong, Y. (2013) Signaling pathways that control cell proliferation. *Cold Spring Harb. Perspect. Biol.* **5,** a008904

21. Weedon-Fekjær, M. S., and Taskén, K. (2012) Review: spatiotemporal dynamics of hCG/cAMP signaling and regulation of placental function. *Placenta* **33,** S87-S91
22. Naderi, S., Wang, J. Y., Chen, T. T., Gutzkow, K. B., and Blomhoff, H. K. (2005) cAMP-mediated inhibition of DNA replication and S phase progression: involvement of Rb, p21Cip1, and PCNA. *Mol. Biol. Cell* **16,** 1527–1542
23. Ward, A. C., Csar, X. F., Hoffmann, B. W., and Hamilton, J. A. (1996) Cyclic AMP inhibits expression of D-type cyclins and cdk4 and induces p27Kip1 in G-CSF-treated NFS-60 cells. *Biochem. Biophys. Res. Commun.* **224,** 10–16
24. Ferretti, C., Bruni, L., Dangles-Marie, V., Pecking, A. P., and Bellet, D. (2007) Molecular circuits shared by placental and cancer cells, and their implications in the proliferative, invasive and migratory capacities of trophoblasts. *Hum. Reprod. Update* **13,** 121–141
25. Huang, Q., Li, J., Wang, F., Oliver, M. T., Tipton, T., Gao, Y., and Jiang, S. W. (2013) Syncytin-1 modulates placental trophoblast cell proliferation by promoting G_1/S transition. *Cell Signal.* **25,** 1027–1035
26. Gündisch, S., Boeckeler, E., Behrends, U., Amtmann, E., Ehrhardt, H., and Jeremias, I. (2012) Glucocorticoids augment survival and proliferation of tumor cells. *Anticancer Res.* **32,** 4251–4261
27. Rabbitt, E. H., Ayuk, J., Boelaert, K., Sheppard, M. C., Hewison, M., Stewart, P. M., and Gittoes, N. J. (2003) Abnormal expression of 11 β-hydroxysteroid dehydrogenase type 2 in human pituitary adenomas: a prereceptor determinant of pituitary cell proliferation. *Oncogene* **22,** 1663–1667
28. Naderi, S., Gutzkow, K. B., Låhne, H. U., Lefdal, S., Ryves, W. J., Harwood, A. J., and Blomhoff, H. K. (2004) cAMP-induced degradation of cyclin D3 through association with GSK-3β. *J. Cell Sci.* **117,** 3769–3783
29. Williamson, E. A., Burgess, G. S., Eder, P., Litz-Jackson, S., and Boswell, H. S. (1997) Cyclic AMP negatively controls c-myc transcription and G_1 cell cycle progression in p210 BCR-ABL transformed cells: inhibitory activity exerted through cyclin D1 and cdk4. *Leukemia* **11,** 73–85
30. Ni, X. T., Duan, T., Yang, Z., Guo, C. M., Li, J. N., and Sun, K. (2009) Role of human chorionic gonadotropin in maintaining 11β-hydroxysteroid dehydrogenase type 2 expression in human placental syncytiotrophoblasts. *Placenta* **30,** 1023–1028
31. Conradt, E., Lester, B. M., Appleton, A. A., Armstrong, D. A., and Marsit, C. J. (2013) The roles of DNA methylation of NR3C1 and 11β-HSD2 and exposure to maternal mood disorder *in utero* on newborn neurobehavior. *Epigenetics* **8,** 1321–1329
32. Jensen Peña, C., Monk, C., and Champagne, F. A. (2012) Epigenetic effects of prenatal stress on 11β-hydroxysteroid dehydrogenase-2 in the placenta and fetal brain. *PLoS ONE* **7,** e39791
33. Zhao, Y., Gong, X., Chen, L., Li, L., Liang, Y., Chen, S., and Zhang, Y. (2014) Site-specific methylation of placental HSD11B2 gene promoter is related to intrauterine growth restriction. *Eur. J. Hum. Genet.* **22,** 734–740
34. Fogarty, N. M., Burton, G. J., and Ferguson-Smith, A. C. (2015) Different epigenetic states define syncytiotrophoblast and cytotrophoblast nuclei in the trophoblast of the human placenta. *Placenta* **36,** 796–802
35. Rugg-Gunn, P. J. (2012) Epigenetic features of the mouse trophoblast. *Reprod. Biomed. Online* **25,** 21–30
36. Rugg-Gunn, P. J., Cox, B. J., Ralston, A., and Rossant, J. (2010) Distinct histone modifications in stem cell lines and tissue lineages from the early mouse embryo. *Proc. Natl. Acad. Sci. U.S.A.* **107,** 10783–10790
37. Zuo, R. J., Gu, X. W., Qi, Q. R., Wang, T. S., Zhao, X. Y., Liu, J. L., and Yang, Z. M. (2015) Warburg-like glycolysis and lactate shuttle in mouse decidua during early pregnancy. *J. Biol. Chem.* **290,** 21280–21291
38. Zhang, N., Wang, W., Li, W., Liu, C., Chen, Y., Yang, Q., Wang, Y., and Sun, K. (2015) Inhibition of 11β-HSD2 expression by triclosan via induction of apoptosis in human placental syncytiotrophoblasts. *J. Clin. Endocrinol. Metab.* **100,** E542–549
39. Wang, W., Guo, C., Zhu, P., Lu, J., Li, W., Liu, C., Xie, H., Myatt, L., Chen, Z. J., and Sun, K. (2015) Phosphorylation of STAT3 mediates the induction of cyclooxygenase-2 by cortisol in the human amnion at parturition. *Sci. Signal.* **8,** ra106